Supporting Information

Kim *et al.* 10.1073/pnas.0802460105

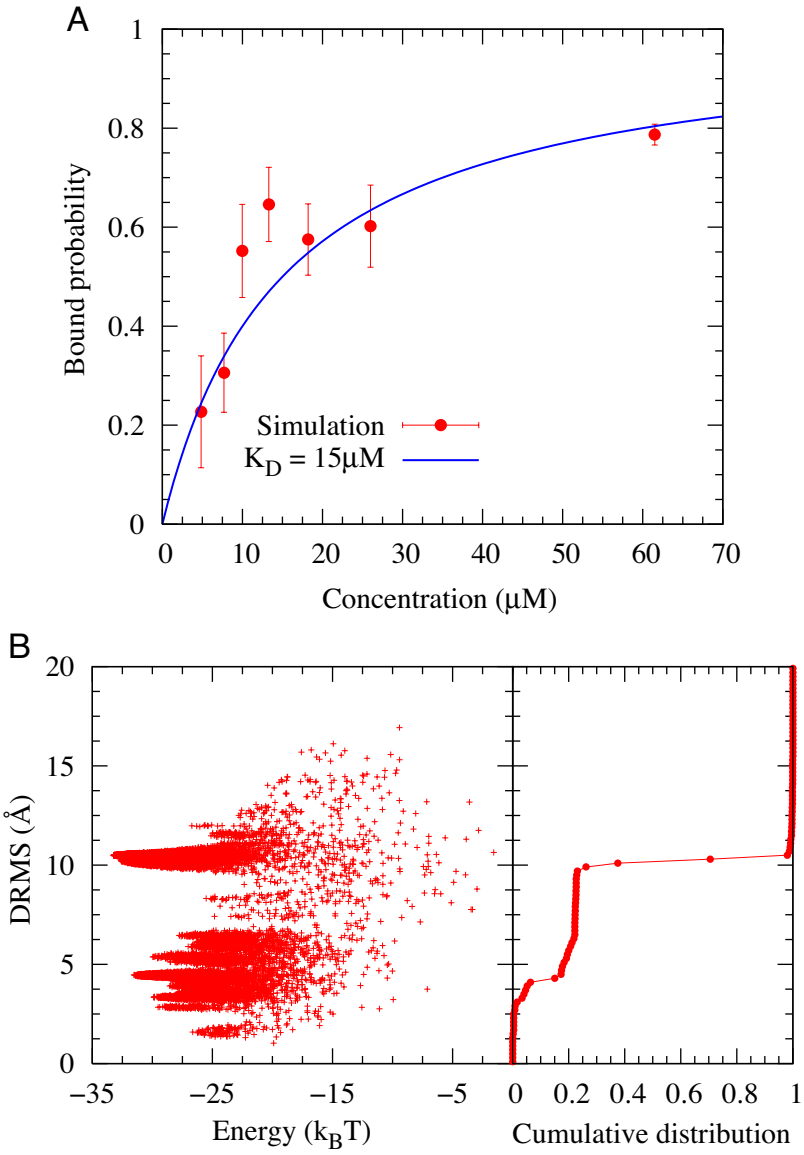

Fig. S1. IIA^{Mtl}-HPr complex affinity and structure. (*A*) Fraction of bound states as a function of protein concentration from the REMC simulations. The solid curve is a titration fit with $K_D = 15\ \mu M$. (*B*) Scatter plot of DRMS versus energy and the corresponding DRMS cumulative distribution.

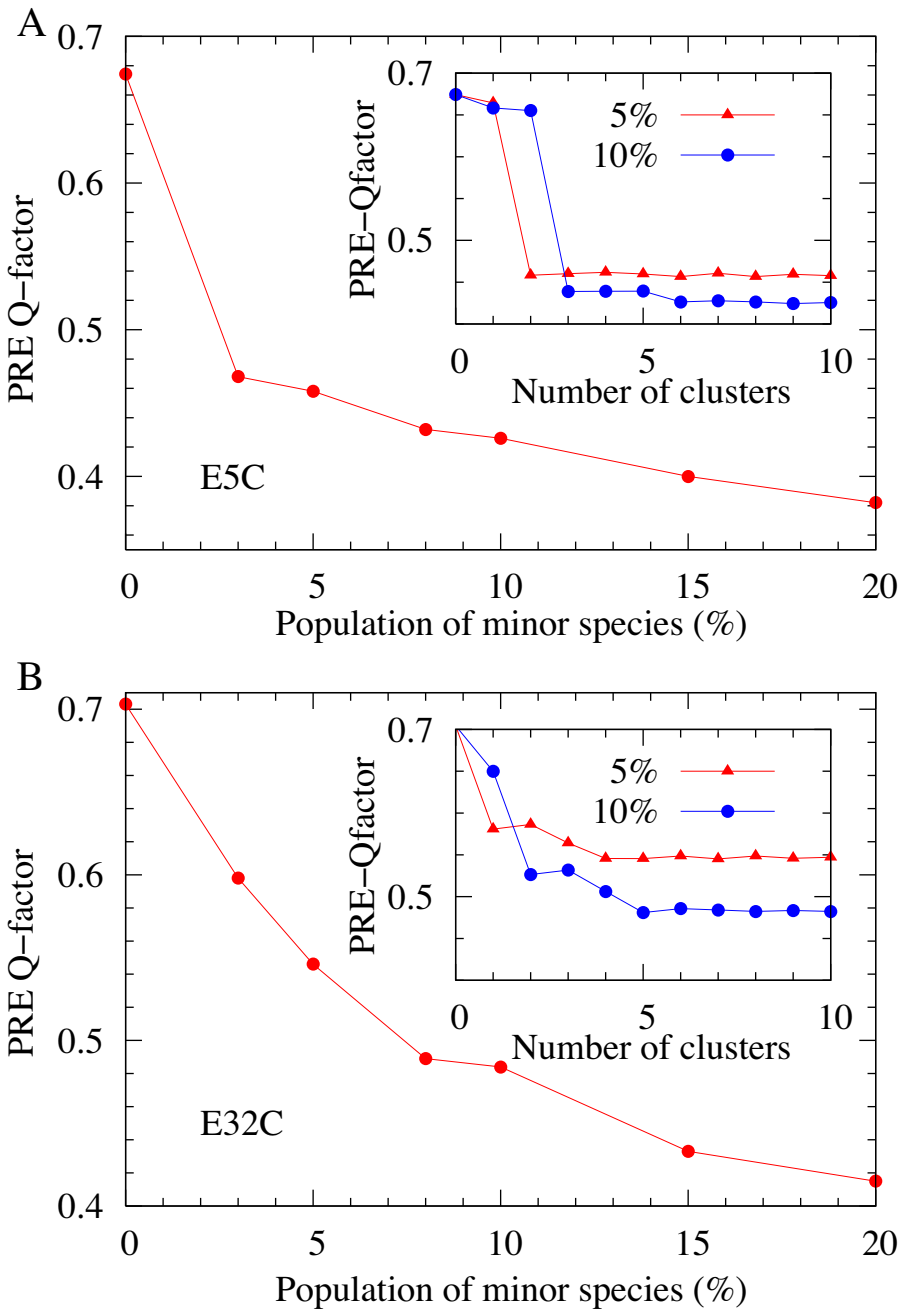

Fig. S2. PRE *Q*-factor for the EIN-HPr complex as a function of the population of nonspecific complexes for EDTA-Mn^{2+} attached to E5C (*A*) and E32C (*B*) sites. (*Insets*) PRE Q-factors as a function of the number of clusters at p_{minor} = 5 and 10%.

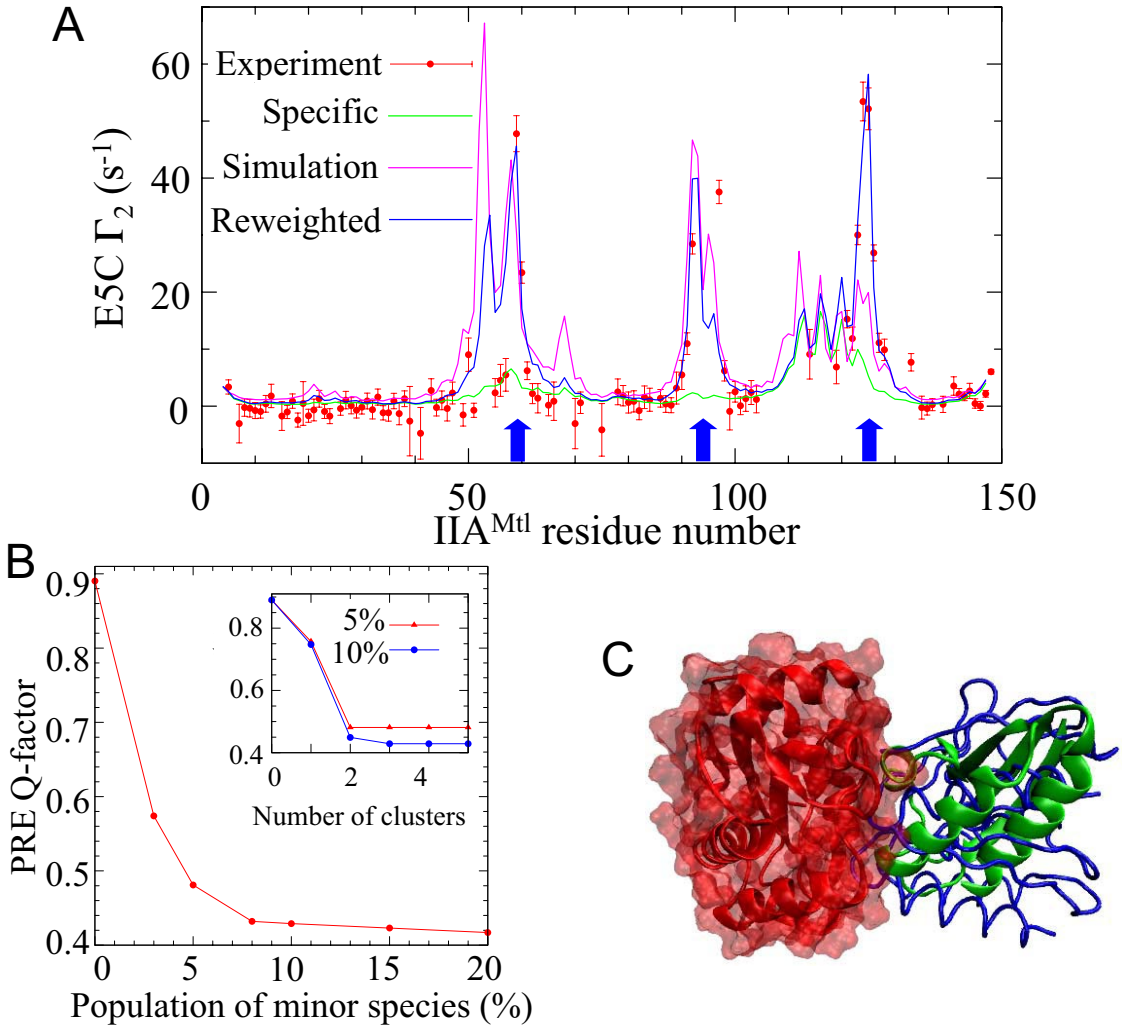

Fig. S3. IIA^{Mtl}-HPr(E5C) complex. (*A*) Observed (red circles), simulated (purple), and reweighted (blue) intermolecular PRE rates Γ_2 for the IIA^{Mtl}-HPr complex with EDTA-Mn^{2+} attached to the E5C site on HPr. For comparison, PREs calculated from the stereospecific complex alone are shown in green. Note that the cutoff distance between Mn^{2+} coordinates and residues of IIA^{Mtl} is 15 Å. (*B*) PRE *Q*-factor as a function of the population of nonspecific complexes, p_{minor}. (*Inset*) PRE *Q*-factor as a function of the number of clusters at $p_{minor} = 5\%$ and 10%. (*C*) Structures of the stereospecific complex (green) and transient encounter complex (blue). IIA^{Mtl} is colored in red.

Table S1. Distances (in Å) from a three-conformer representation of Mn^{2+} to three consecutive C^{α} atoms with the one to which the paramagnetic label is attached in the middle

Residue no.	E5C			Residue no.	E25C			Residue no.	E32C		
4	8.2	11.2	9.3	24	8.7	9.2	12.0	31	13.0	13.4	11.2
5	6.4	8.1	10.5	25	5.4	5.8	9.7	32	9.4	9.7	7.6
6	5.0	9.5	14.2	26	8.1	8.4	13.1	33	9.7	10.2	8.9

Other Supporting Information Files

Appendix (PDF)